

# Assessment of Beam Damage in Polymers Caused by in situ ESEM Analysis using IR Spectroscopy

Armin Zankel,<sup>\*1</sup> Borisl Chernev,<sup>1</sup> Christian Brandl,<sup>1</sup> Peter Poelt,<sup>1</sup> Peter Wilhelm,<sup>1</sup> Michael Nase,<sup>2,4</sup> Beate Langer,<sup>2</sup> Wolfgang Grellmann,<sup>2,3</sup> Hans Joachim Baumann<sup>4</sup>

**Summary:** The environmental scanning electron microscope (ESEM) enables in situ analyses of non-conducting samples such as polymers, thus allowing microscopic phenomena to be correlated to macroscopic measurement data. Unfortunately, irradiation of polymers with electrons always causes beam damage<sup>[1]</sup> and it is unclear whether this damage could influence the outcome of the experiments. The amount of beam damage in polymers is mainly determined by the electron dose, which is a function of the probe current, the irradiation time, the irradiated area and the type of imaging gas used. The beam damage during in situ tensile tests of peel films was assessed using Fourier transformed infrared spectroscopy (FTIR). The band at  $965\text{ cm}^{-1}$  turned out to be significant for the estimation of beam damage in this material, which was verified by long-term measurements. The measurements were performed in an ESEM Quanta 600 FEG at parameters comparable to the prior in situ tensile tests. Additional measurements were performed in a Quanta 200 at parameters typical of in situ investigations. Again, the out-of-plane trans =C–H wag at  $965\text{ cm}^{-1}$  turned out to be significant for beam damage and was used as an indicator for beam damage (dehydrogenation) for this type of material.

**Keywords:** electron beam irradiation; ESEM; FT-IR; peel test; PE/PB-1 blends

## Introduction

The environmental scanning electron microscope (ESEM) enables in situ investigations of non-conducting specimens, thus allowing microscopic phenomena to be correlated with macroscopic measurement data. The principle of in situ tensile testing of polymers in the ESEM is described in<sup>[2]</sup> and results of in situ tensile tests of polyethylene/polybutene-1 (PE/PB-1) – peel systems in the ESEM have been published in<sup>[3]</sup>.

Figure 1 shows a photograph of the setup of the tensile stage mounted on the microscope stage of an ESEM Quanta

600 FEG equipped with a Schottky emitter (FEI Company, Eindhoven, The Netherlands). T-peel tests<sup>[4]</sup> on polymer films were performed, at which the ends of the films were pulled apart with a constant clamp velocity of 1 mm/min using a motor. The T-geometry of the peel film was stabilized in a brass groove in order to emulate the characteristics of a classical T-peel test. During tensile testing, the cracks were imaged in situ with the microscope, with this type of setup enabling an excellent insight into the crack region during the recording of the whole force displacement curve (peel curve).

The imaging principle of the ESEM is fundamental for these tests as it allows the investigation of electrically non-conducting specimens without the necessity of a conductive coating.

This is achieved by a vacuum which is lower than in the conventional SEM,

<sup>1</sup> Institute for Electron Microscopy, Graz University of Technology, Steyrergasse 17, A-8010 Graz, Austria  
E-mail: armin.zankel@felmi-zfe.at

<sup>2</sup> Polymer Service GmbH Merseburg, Germany

<sup>3</sup> Martin Luther University of Halle-Wittenberg, Centre of Engineering, Germany

<sup>4</sup> ORBITA-FILM GmbH, Germany

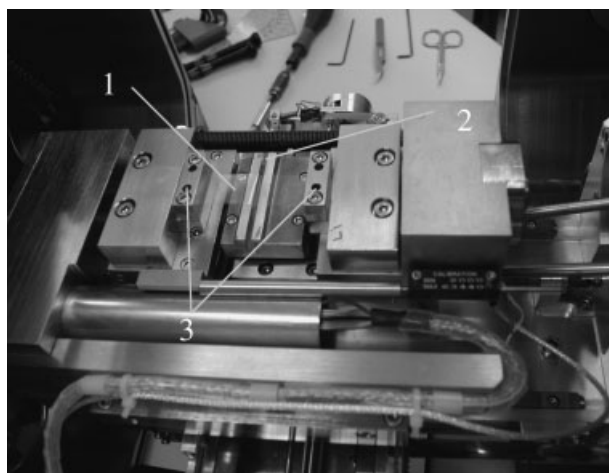


**Figure 1.**

Tensile stage mounted on the microscope stage of the ESEM Quanta 600 FEG. 1: peel film; 2: groove; 3: clamps.

where typically a vacuum of about  $10^{-5}$  torr (1 torr = 133 Pa) is maintained.

A pressure between 0.08 and 1 torr can be chosen in the low vacuum mode of the ESEM,<sup>[5]</sup> thereby avoiding charging of the specimen surface.

The schematic in Figure 2 shows the interaction between the electrons accelerated to the detector and the gas molecules. The accelerated electrons collide with gas molecules, thus inducing ionization processes. These processes produce new electrons, called environmental secondary electrons,<sup>[6]</sup> and positive ions. This process is repeated many times between the surface

of the specimen and the detector electrode, leading to a proportional cascade amplification of the original secondary electron signal.<sup>[7]</sup>

The ionization processes provide a double benefit for imaging. Firstly, the interesting signal is amplified thus enhancing the SNR, and secondly, positive ions are swept towards the surface of the specimen and neutralize the negative charges on the surface. This is the reason why ESEM allows stable imaging of non-conducting specimens.

However, it is well-known that imaging of polymers with electrons can cause beam damage, since the impinging electrons can

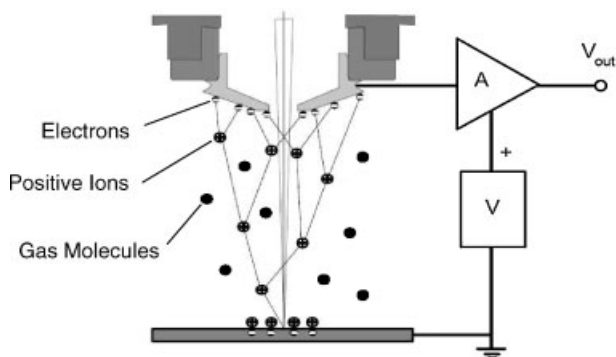


**Figure 2.**

Schematic of an environmental secondary electron detector.<sup>[7]</sup>

modify the material's morphology as well as its chemistry.<sup>[8,9]</sup>

## Material and Methods

Peel films and peel systems are a growing field in the packaging industry. Examples of the wide use of these systems include food packaging, medical cutlery and multipurpose wrapping.<sup>[10]</sup>

Aside from the daily use of these systems in the household, they are indispensable in the field of medicine for objects like cutlery, catheters or prostheses, where quick and sterile handling without the use of a supporting tool is a necessity.<sup>[11]</sup>

It is not only a question of ease and hygiene in handling but also important for systematic working, to determine and present the fracture behavior of such films in a well designed manner. The following aspects are important for usage: Constant force during the tearing open, small peel forces and fracture at well designed regions of the wrap.

These properties can be determined by the material itself, the conditions during processing of the material and the parameters governing the production of the wrap.

Common peel film systems are based on a matrix-particle structure and thus consist of two phases. In our case the matrix was polyethylene (PE), with particles of 1-polybutene (PB-1) dispersed in it.

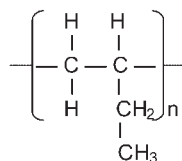


**Figure 3.**  
1-Polybutene (PB-1).

PB-1 is produced by polymerization of 1-butene monomers using a stereospecific Ziegler-Natta catalyst, leading to a linear, isotactic, partially crystalline polymer. Figure 3 shows one unit of the polymer.

Its similar structure to polypropylene makes it compatible with this polymer, whereas it is not compatible with polyethylene. PB-1 copolymers are used in several types of PE foils as a matrix component in order to lower adhesion.<sup>[12]</sup>

Thus the peel effect is determined by the morphology of the material. Figure 4 shows the particle-matrix morphology. The brighter particles show lamellae, which are rather coarse compared to the lamellae of the PE matrix. Typically the particles have diameters of about 50 to 100 nm.

The build-up of a peel film is sketched in Figure 5. The material is sealed at a temperature of about 140 °C (seal pressure 175 kPa, seal time 2 s, cooling time in air 6.5 s). The seal area has a length (L) of 5.5 mm and a width (W) of 15 mm. The forces operate at the peel arms of the film. The fracture behavior is dependent on the angle between the arms of the peel film and

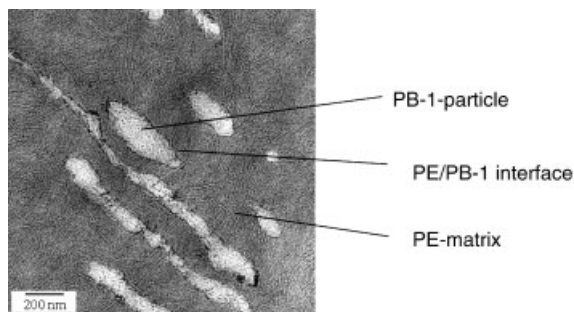


**Figure 4.**

TEM image of the cross-section of a peel film showing the size and distribution of the PB particles in the PE matrix.

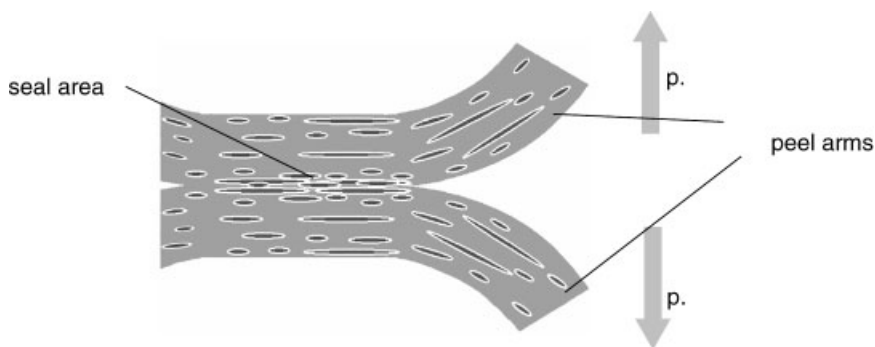


**Figure 5.**

Build-up of a peel film; p.: peel force.

can be investigated in a tensile testing machine equipped with an additional angle adjustment fixture. The angle geometry of  $180^\circ$  between the arms and  $90^\circ$  between the seal area and the arms is called T-peel test setup. A groove (Figure 1) was used to

emulate this geometry for an in situ T-peel test.

Figure 6 shows four micrographs of the crack region of the film during a T-peel test correlated with the force displacement curve (peel curve). The points in the curve

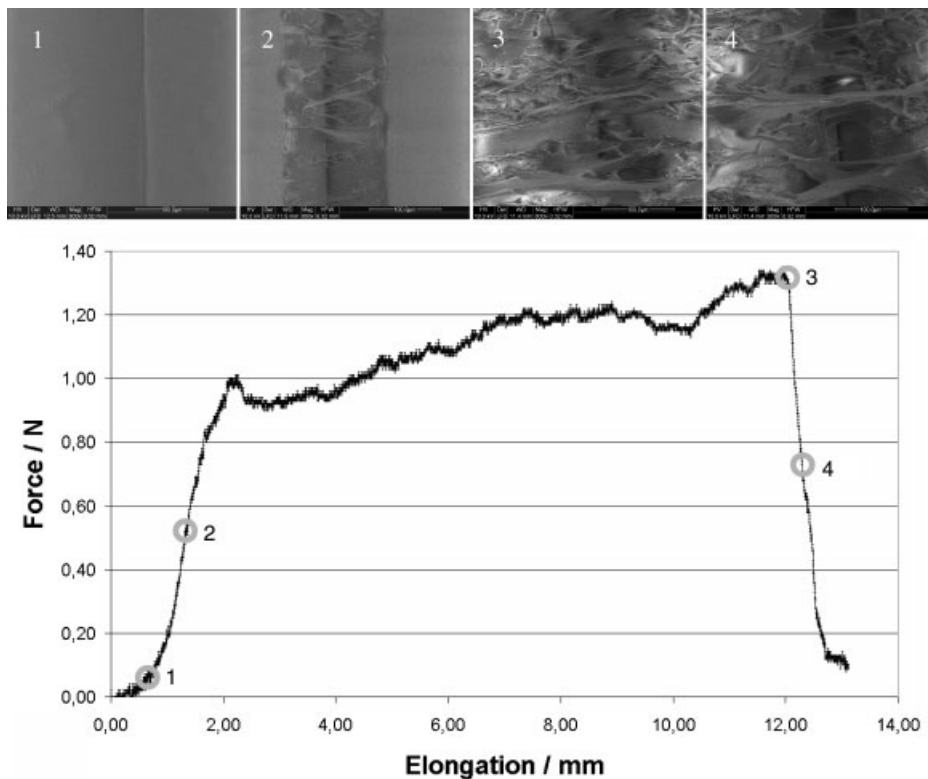


**Figure 6.**

Top: ESEM images recorded at the points marked in the force; bottom: elongation diagram of the corresponding peel test.

indicate the elongations at which the respective micrographs were recorded.

The correlation between the micrographs and the peel curve gives the opportunity to investigate the crack propagation through the material. Several types of fibrillation of the material can be found, depending on the amounts of polybutene in the matrix. The difference between interlaminar and intralaminar fracture<sup>[13,14]</sup> can be observed in situ.

But unfortunately, irradiation of polymers with electrons always causes damage to the polymers<sup>[1]</sup> and it is unclear whether this damage could influence the outcome of the experiments.

The time of exposure of the peel film was measured for assessing beam damage during in situ tensile tests using Fourier transformed infrared spectroscopy (FTIR). Subsequently, the peel films were irradiated for the same length of time with the same probe current.

The current was measured before and after the peel test and also during the irradiation experiment by use of a Faraday cup, which was mounted on the microscope stage, and an ammeter (Keithley 616 Digital Electrometer). A current of about 0.4 nA was measured.

In addition to the experiments in the ESEM Quanta 600 FEG (electron source: Schottky emitter), similar measurements were performed in an ESEM Quanta 200 (electron source: tungsten filament). The dependence of specimen degradation on some of the operating parameters of the microscope was also investigated.

FTIR measurements were performed in micro-ATR (attenuated total reflection) mode, using a Bruker Hyperion 3000 infrared microscope, coupled to a Bruker Equinox 55 FTIR spectrometer. The used 20×  $\mu$ -ATR objective was equipped with a Ge crystal and an electronic pressure control system, assuring the reproducibility of the single measurements. The spectra were recorded in the spectral region 4000–500  $\text{cm}^{-1}$ , spectral accumulation of 32 single scans with spectral resolution of 4  $\text{cm}^{-1}$ . The evaluation of the spectra was

carried out using the OPUS<sup>®</sup> software package (Bruker Optics GmbH).

## Results

### Investigation of Beam Damage in the ESEM Quanta 600 FEG

For the estimation of the beam damage with Fourier transformed infrared spectroscopy (FTIR) the polymer surfaces were irradiated in the ESEM using the same parameters as for the tensile tests, i.e. electron energy: 10 keV, probe current: 0.4 nA, pressure of the imaging gas (water vapor): 0.5 torr, field width of the irradiated area: 160  $\mu\text{m}$  and 320  $\mu\text{m}$ . The FTIR spectra of peel films with a polybutene content of 6% (PE + 6 wt-%PB-1) are depicted in Figure 7. Figure 7a shows the spectrum of an unirradiated film, while Figure 7b and 7c depict the spectra of irradiated films, with an area of a width of 160  $\mu\text{m}$  irradiated for 15 s and an area with a width of 320  $\mu\text{m}$  irradiated for 30 s, respectively. The colored region indicates the integration area for the calculation of the integral intensity.

The spectra demonstrate that nearly the same integral absorption was obtained for the two irradiated films. Since the integral absorption of the correlated band is low relative to other bands of polyethylene, the beam damage of the film at the parameters used can be regarded as very small.

The absorption was measured at a band of 965  $\text{cm}^{-1}$ , because the respective spectra show no alteration at other wave numbers with changing electron doses. Consequently, the out-of-plane trans =C–H wag at 965  $\text{cm}^{-1}$  was used as an indicator for beam damage (dehydrogenation) in this type of material.

This was verified by long-term measurements, where longer irradiation times correlated with a stronger absorption at 965  $\text{cm}^{-1}$ .

Figure 8 presents three spectra, which show an increase in beam damage by a growth of the respective IR band. The first spectrum is that of an unirradiated film (PE + 6 wt-%PB-1), the second that of a

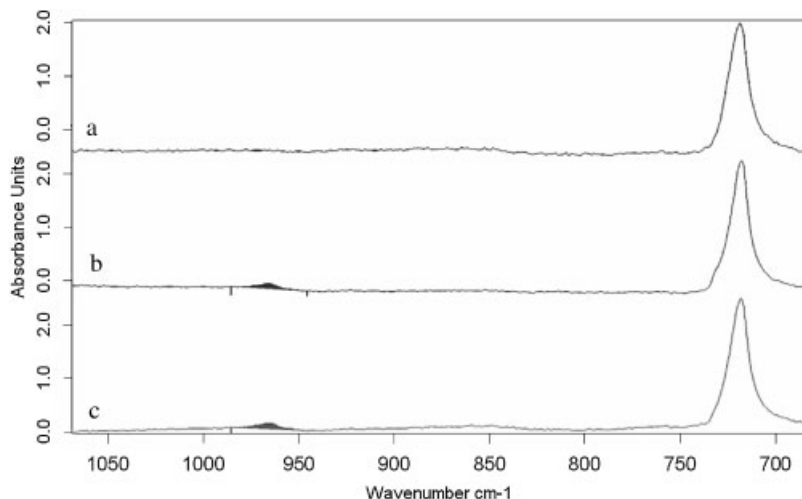


**Figure 7.**

Infrared spectra of the surface of a peel film (PE + 6 wt-%PB-1); a: not irradiated; b: irradiation of an area with a width of 160  $\mu\text{m}$  for 15 s; c: irradiation of an area of a width of 320  $\mu\text{m}$  for 30 s (the y-axis was scaled with respect to the height of the band at 720  $\text{cm}^{-1}$ ).

film irradiated for 30 s and the third that of a film irradiated for 10 minutes. A strong increase in the marked absorption band with increasing irradiation time can be observed.

Based on these results, the irradiation damage of peel films was more extensively investigated in an ESEM Quanta 200 with a

tungsten filament at parameters typical of in situ investigations.

#### Investigation of Beam Damage in the ESEM Quanta 200

Specimen degradation caused by the electron irradiation was investigated as a

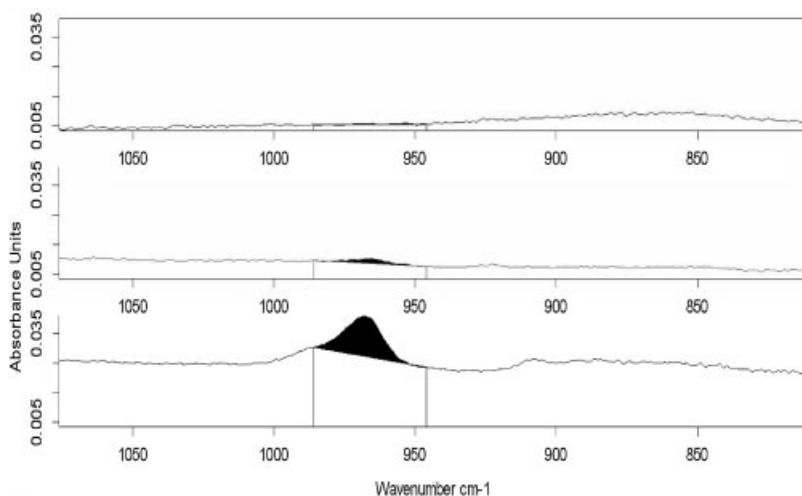


**Figure 8.**

Infrared spectra of the surfaces of peel films (PE + 6 wt-%PB-1); a: unirradiated; b: irradiation for 30 s; c: irradiation for 10 min (the y-axis was scaled with respect to the height of the band at 965  $\text{cm}^{-1}$ ).

function of irradiation time, pressure in the microscope chamber and electron energy for peel films with a polybutene content of 3% (PE + 3 wt-%PB-1) and 15% (PE + 15 wt-%PB-1).

#### Variation of Pressure

The pressure of the imaging gas (water vapor) was varied, with all the other parameters kept constant (electron energy: 10 keV, irradiation time: 30 s, probe current: about 0.04 nA). A varying gas pressure in the microscope chamber also causes a variation in the electron dose. Part of the electrons are scattered out of the beam by the interactions with the gas atoms or molecules (skirt effect<sup>[9]</sup>), reducing the number of electrons and thus the electron dose at the impact point of the residual focused beam.

The simulations in Figure 9 show this skirt effect for pressures of 0.4, 0.7 and 1 torr, with water vapor as the imaging gas. At 0.4 torr 82% of the electrons are unscattered, followed by 72% at 0.7 torr and 62% at 1 torr.

The infrared spectra in Figure 10 prove by the absence of the absorption peak at  $965\text{ cm}^{-1}$ , that no measurable irradiation damage occurred, not even at the lowest gas pressure.

Thus, in contrast to the experiments in the Quanta 600 FEG, no irradiation damage was detected. This can be explained by the much lower probe current and thus lower electron dose than in the ESEM Quanta 600 experiments as well as the lower brightness and larger diameter of beams generated by a tungsten filament in comparison to a Schottky emitter. But this demonstrates that, at least for

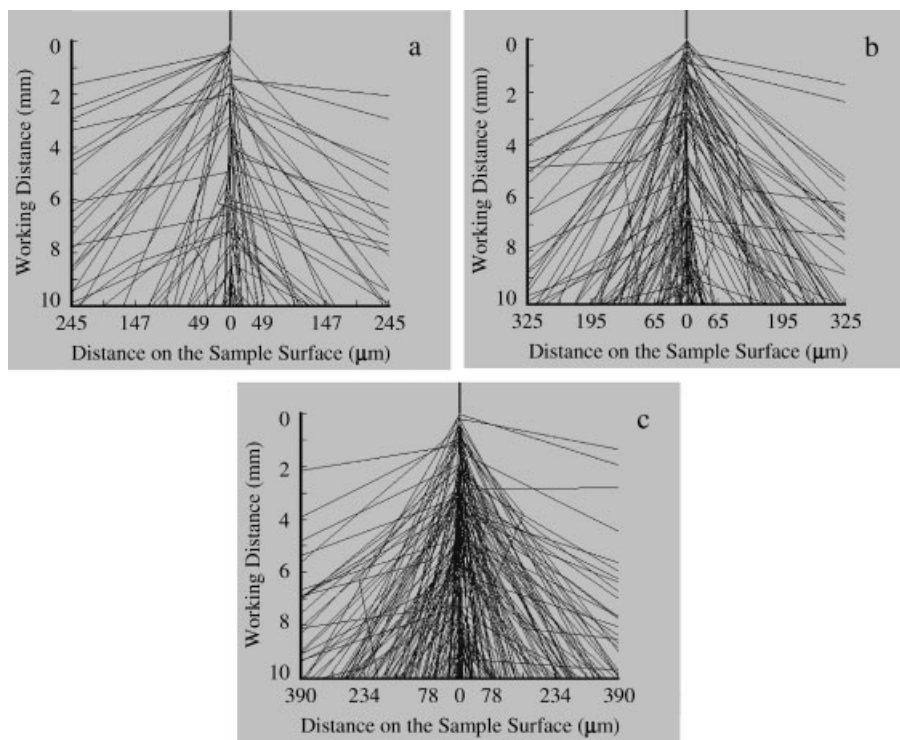


**Figure 9.**

Simulations of the skirt effect at various pressures in an ESEM using the program “Electron Flight Simulator<sup>TM</sup>” (Small World); parameters: gas: water vapor, working distance 10 mm, electron energy: 10 keV pressure: a: 0.4 torr, b: 0.7 torr, c: 1.0 torr.



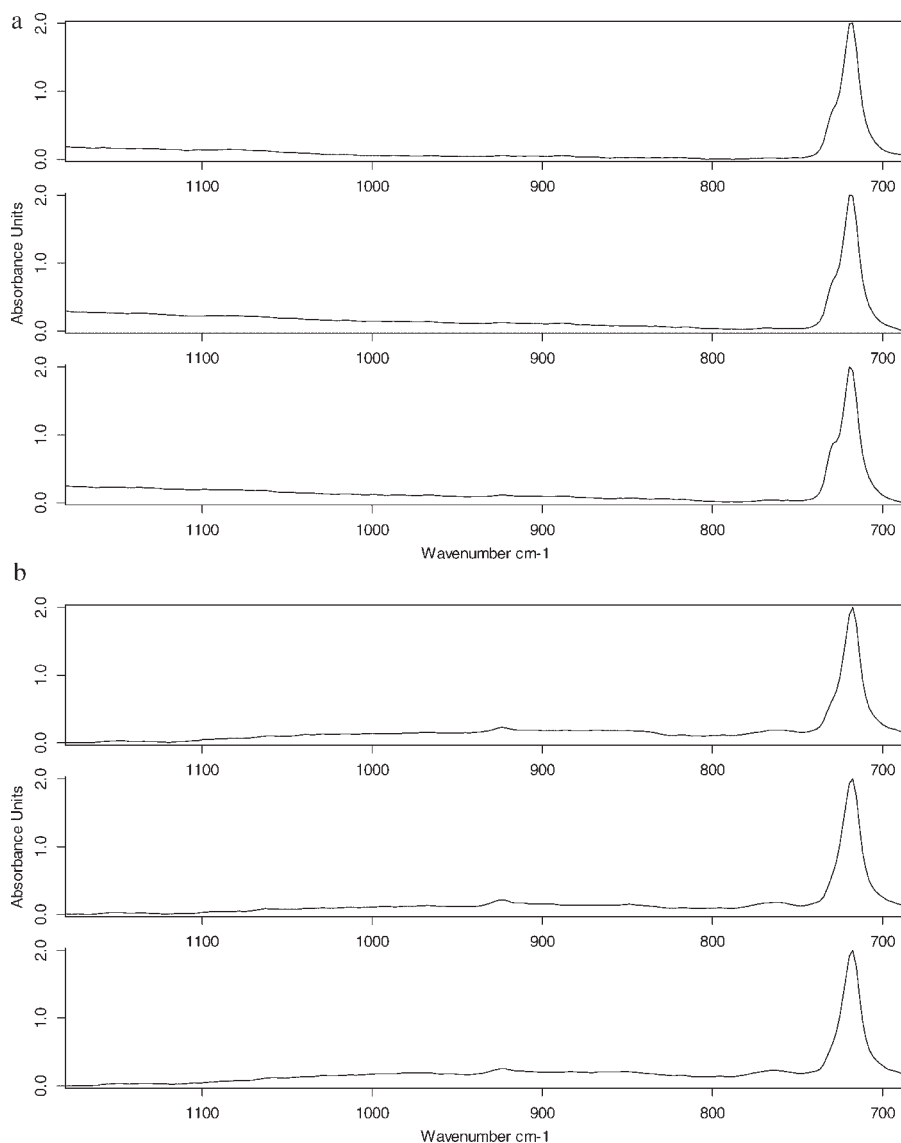


**Figure 10.**

Infrared spectra of the surfaces of peel films (a: PE + 3 wt-%PB-1, b: PE + 15 wt-%PB-1), with the pressure in the microscope chamber varied: from top to bottom: 0.4, 0.7, 1.0 torr.

this type of material, a threshold for the electron dose exists below which no measurable material degradation can be observed by IR.

#### *Variation of Irradiation Time*

However, a strong dependence on the irradiation times and the electron energy

was found at higher doses (Figure 11, Figure 12).

Figure 11a shows five spectra of peel films with a polybutene content of 3% (PE + 3 wt-%PB-1), with the beam damage plotted as a function of time.

The difference in the height of the absorption peaks in Figure 11b and 11c



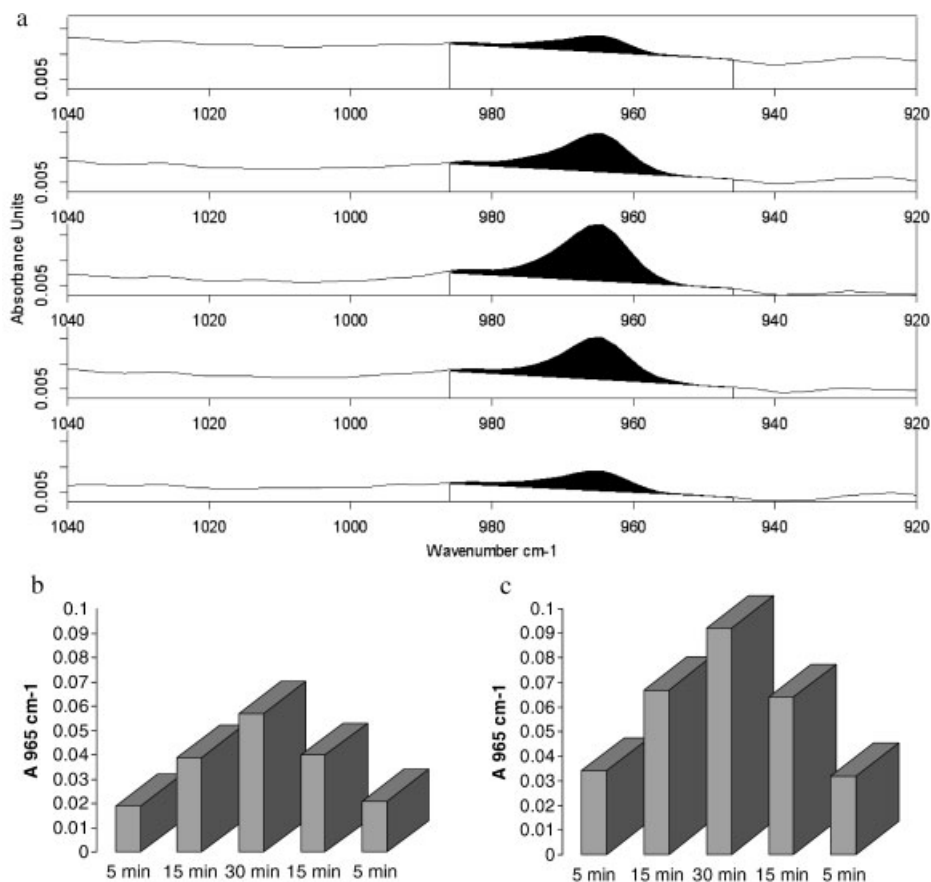


**Figure 11.**

a: Infrared spectra with the corresponding integration regions for determining integral absorption (PE + 3 wt-%PB-1; irradiation time: 5, 15, 30, 15, 5 min; probe current: 0.021 nA, y-axis: arbitrary units, same scaling for all five spectra); b: integral absorption as a function of the irradiation time (PE + 3 wt-%PB-1; 5, 15, 30, 15, 5 min; probe current: 0.021 nA); c: integral absorption as a function of the irradiation time (PE + 15 wt-%PB-1; 5, 15, 30, 15, 5 min; probe current: 0.032 nA).

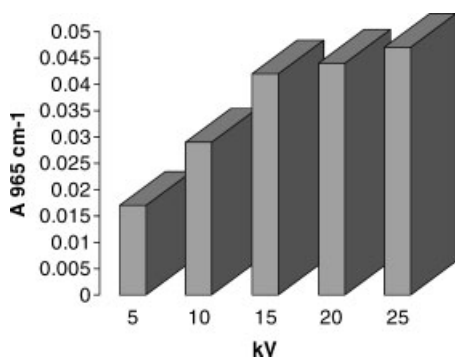


**Figure 12.**

Dependence of material degradation on the electron energy.

can be explained by the difference in the probe currents (Figure 11b 0.021 nA, Figure 11c 0.032 nA) at which the two investigations were performed. The electron energy was 10 keV in all cases.

#### Variation of Electron Energy

First measurements of the beam damage at different electron energies confirm that the peak at 965 cm<sup>-1</sup> in the IR spectrum is significant for the evaluation of beam damage in this type of polymer even at higher energies. The integral absorption

in dependence on the electron energy is shown in Figure 12.

It is obvious that beam damage increases monotonically with the electron energy, showing saturation at higher energies.

## Conclusion

Fourier transformed infrared spectroscopy (FTIR) was used for the estimation of the beam damage caused by the electron irradiation of peel films during investigations in the environmental scanning electron microscope (ESEM). The films consisted of a polyethylene/polybutene-1 blend. Several parameters were varied to figure out at which parameters the investigation of this material can be performed with minimum beam damage. No measurable degradation of the material was observed for low electron doses.

The absorption band at  $965\text{ cm}^{-1}$  turned out to be significant for the estimation of beam damage in this material. This was verified by long-term measurements with high electron doses, which were performed in an ESEM Quanta 600 FEG (electron source: Schottky emitter) under conditions comparable to those used in the peel tests.

Additional measurements in an ESEM Quanta 200 (electron source: tungsten filament) were also performed under conditions typical for in situ analyses. Once more the  $965\text{ cm}^{-1}$  out-of-plane trans

=C–H wag, due to dehydrogenation, was identified as a marker for beam damage.

- [1] R. F. Egerton, P. Li, M. Malac, *Micron* **2004**, 35, 399.
- [2] A. Zankel, P. Poelt, M. Gahleitner, E. Ingolic, *Scanning* **2007**, 29, 261.
- [3] M. Nase, A. Zankel, B. Langer, H. Baumann, W. Grellmann, *Scanning* **2007**, 29, 50.
- [4] W. Grellmann, B. Langer, M. Nase, H. Baumann, International Conference "Werkstoffprüfung 2006 – Fortschritte der Kennwertermittlung für Forschung und Praxis", Conference Proceedings, **2006**, 439.
- [5] D. J. Stokes, *Science, Technology and Education of Microscopy* **2006**, 564, <http://www.formatex.org/microscopy/content.htm>.
- [6] A. L. Fletcher, B. L. Thiel, A. M. Donald, *J. Phys. D: Appl. Phys.* **1997**, 30, 2249.
- [7] FEI, Philips Electron Optics, Eindhoven, The Netherlands, "Environmental Scanning Electron Microscopy, An Introduction to ESEM<sup>TM</sup>", Robert Johnson Associates **1996**.
- [8] L. C. Sawyer, D. T. Grubb, "Polymer Microscopy", 2<sup>nd</sup> ed., Chapman and Hall, New York **1996**.
- [9] J. I. Goldstein, D. E. Newbury, P. Echlin, D. C. Joy, C. E. Lyman, E. Lifshin, L. Sawyer, J. R. Michael, "Scanning Electron Microscopy and X-Ray Microanalysis", 3<sup>rd</sup> ed., Kluwer Academic/Plenum Publishers, New York **2003**.
- [10] W. Grellmann, "Mechanische Kunststoffprüfung", manual of the VDI-tutorial Nr. 356205, **2006**.
- [11] P. Stober, H. Rist, *Kunststoffe* **2004**, 6, 66.
- [12] F. Schemm, F. Van de Vliet, J. Grasmeder, Polybuten (PB-i) – Faszinierendes Polyolefin, 7. Kunststoffrohrtage in Würzburg, Conference Proceedings **2001**, pp. 1ff.
- [13] M. Nase, R. Androsch, B. Langer, H. Baumann, W. Grellmann, *J Polym Sci* **2008**, 107, 3111.
- [14] M. Nase, B. Langer, H. Baumann, W. Grellmann, International Conference "Polymerwerkstoffe 2006", Conference Proceedings, **2006**, 56.